

HIGH ORDER VEM ON CURVED DOMAINS.

SILVIA BERTOLUZZA, MICOL PENNACCHIO, AND DANIELE PRADA

ABSTRACT. We deal with the virtual element method (VEM) for solving the Poisson equation on a domain Ω with curved boundaries. Given a polygonal approximation Ω_h of the domain Ω , the standard order m VEM [6], for m increasing, leads to a suboptimal convergence rate. We adapt the approach of [14] to VEM and we prove that an optimal convergence rate can be achieved by using a suitable correction depending on high order normal derivatives of the discrete solution at the boundary edges of Ω_h , which, to retain computability, is evaluated after applying the projector Π^∇ onto the space of polynomials. Numerical experiments confirm the theory.

1. INTRODUCTION

The virtual element method (VEM) is a PDE discretization framework designed to easily handle meshes consisting of very general polygonal or polyhedral elements [4]. The method can be considered as a generalization of the Finite Element Method (FEM) to polytopal tessellations, in that it looks for the solution in a conforming discretization space with a Galerkin approach. By giving up conformity in the discretization of the bilinear form corresponding to the differential operator, the method manages to avoid the explicit construction of the basis functions (whence the name *virtual*). Everything is computed directly in terms of the degrees of freedom by resorting to suitable “computable” (in terms of the degrees of freedom) elementwise projectors onto the space of polynomials (see [6]), ultimately allowing to define a discrete bilinear form satisfying polynomial exactness and stability properties which allow to prove optimal error estimate for discretization of (arbitrary) order m . Different model problems have already been tackled by using VEM ([27, 1, 2, 10, 11, 24, 15, 5, 19, 7, 13, 18]), and, while most of the literature deals with the h version of the method, the p and hp versions were also discussed and analyzed ([3, 9, 22]).

In this paper we consider the problem of extending the method to problems in domains with smooth curved boundaries. As it happens in the Finite Element case, the approximation of the curved domain by straight facets introduces an error that, for higher order methods, can dominate the analysis. Different approaches for the accurate treatment of curved domains in the finite element framework can be found in literature, see e.g. [25]. Among the different possible approaches to such a problem, following the guidelines of [14], we choose here to approximate the curved domain Ω with a polygonal domain Ω_h , while compensating for the discrepancy in the geometry by suitably modifying the bilinear form. Complying with the VEM philosophy, the modified bilinear form will retain the property of being computable in terms of the degrees of freedom. Of course, other approaches are possible. In [12] the authors propose a direct definition of a modified virtual element space that accommodates curved elements, whose boundary matches exactly the boundary of Ω . While loosing exact reproduction of polynomials, the resulting method retains optimality and, contrary to the one we propose here, it is immediately well suited to deal with curved interior

Date: May 2, 2022.

Key words and phrases. Virtual Element method, Nitsche’s method, curved domain.

This paper has been realized in the framework of ERC Project CHANGE, which has received funding from the European Research Council (ERC) under the European Unions Horizon 2020 research and innovation programme (grant agreement No 694515), and it was partially supported by INDAM - GNCS.

interfaces. On the other hand, our approach has the advantage of only requiring, for the implementation, minor modifications with respect to the polygonal case. To the best of our knowledge, other numerical methods that can handle curved polytopal meshes are only [17] and [20].

The paper focuses on a simple elliptic model problem in 2D and it is organized as follows. As the projection method of [14] combines Nitsche's technique for imposing non homogeneous boundary conditions [23] with the improved accuracy polygonal domain approximation of [26], we start, in Section 2, to adapt Nitsche's method to the Virtual Element framework and we provide a theoretical analysis of the resulting discretization, proving stability and an error estimate. In Section 3 we introduce and analyze the discretization for the problem on curved domains, proving also in this case stability and optimal error estimate. Finally, in Section 4, we test the method on several test cases, with method of different order. Throughout the paper, we will use the notation $A \lesssim B$ (resp. $A \gtrsim B$) to signify that the quantity A is bounded from above (resp. from below) by a constant C times the quantity B , with C independent of the mesh size parameter h , the diameter h_K the specific shape of the polygon K , but possibly depending on the polynomial order m of the method, and on the shape regularity constant α_0 and α_1 appearing in Assumption 2.1.

2. THE NITSCHÉ'S METHOD IN THE VIRTUAL ELEMENT CONTEXT

Before considering the problem of solving a PDE on a domain with a curved boundary, let us discuss how Nitsche's method for imposing non homogeneous boundary condition [23] can be applied in the context of the virtual element method. Throughout this section let then Ω denote a bounded polygonal domain. To fix the ideas, we consider the following simple model problem:

$$(2.1) \quad -\Delta u = f, \text{ in } \Omega, \quad u = g, \text{ on } \partial\Omega,$$

with $f \in L^2(\Omega)$ and $g \in H^{1/2}(\Omega)$. Assume that we are given a family of quasi uniform tessellations \mathcal{T}_h of Ω into polygonal elements K of diameter $h_K \simeq h$. We make the following standard regularity assumptions on the polygons of the tessellation:

Assumption 2.1. There exists constants $\alpha_0, \alpha_1 > 0$ such that:

- (i) each element $K \in \mathcal{T}_h$ is star-shaped with respect to a ball of radius $\geq \alpha_0 h_K$;
- (ii) for each element K in \mathcal{T}_h the distance between any two vertices of K is $\geq \alpha_1 h_K$.

Under Assumptions 2.1, several bounds hold uniformly in h_K [21]. In particular, in the following we will make use of an inverse inequality on the space \mathbb{P}_m of polynomials of order less than or equal to m : for all $p \in \mathbb{P}_m$ and for all j, k with $0 \leq j \leq k$ it holds that

$$(2.2) \quad \|p\|_{k,K} \lesssim h_K^{j-k} \|p\|_{j,K}.$$

Moreover we will make use of the following trace inequality: for all $\phi \in H^1(K)$ we have

$$(2.3) \quad \|\phi\|_{0,\partial K} \lesssim h_K^{-1/2} \|\phi\|_{0,K} + h_K^{1/2} |\phi|_{1,K}.$$

We will consider the standard order m Virtual Element discretization space ([4]), whose definition we briefly recall. For each polygon $K \in \mathcal{T}_h$ we let the space $\mathbb{B}_m(\partial K)$ be defined as

$$\mathbb{B}_m(\partial K) = \{v \in C^0(\partial K) : v|_e \in \mathbb{P}_m \ \forall e \in \mathcal{E}^K\},$$

where \mathcal{E}^K denotes the set of edges of the polygon K . We introduce the local VE space as:

$$V^{K,m} = \{v \in H^1(K) : v|_{\partial K} \in \mathbb{B}_m(\partial K), \ \Delta v \in \mathbb{P}_{m-2}(K)\}$$

(with $\mathbb{P}_{-1} = \{0\}$). The global discrete VE space V_h is then defined as

$$(2.4) \quad \begin{aligned} V_h &= \{v \in H^1(\Omega) : v|_K \in V^{K,m} \ \forall K \in \mathcal{T}_h\} = \\ &= \{v \in H^1(\Omega) : \forall K \in \mathcal{T}_h \ v|_{\partial K} \in \mathbb{B}_m(\partial K), \ \Delta v|_K \in \mathbb{P}_{m-2}(K)\}. \end{aligned}$$

A function in V_h is uniquely determined by the following degrees of freedom

- its values at the vertices of the tessellation;
- (only for $m \geq 2$) for each edge e , its values at the $m - 1$ internal points of the $m + 1$ -points Gauss-Lobatto quadrature rule on e ;
- (only for $m \geq 2$) for each element K , its moments in K up to order $m - 2$.

For any given function $w \in H^2(\Omega)$ we can then define the unique function $w_I \in V_h$ such that: a) the values of w and w_I at the vertices of the tessellation coincide; b) for each edge e , the values of w and w_I at the $m - 1$ internal points of the $m + 1$ -points Gauss-Lobatto quadrature rule on e coincide; c) for each element K , the moments up to order $m - 2$ of w and w_I in K coincide. The function w_I satisfies the following local approximation bound [4]: if $w \in H^s(K)$, with $2 \leq s \leq m + 1$, then

$$(2.5) \quad \|w - w_I\|_{0,K} + h_K |w - w_I|_{1,K} \lesssim h_K^s |w|_{s,K}.$$

Let now

$$a(\phi, \psi) = \int_{\Omega} \nabla \phi \cdot \nabla \psi, \quad a^K(\phi, \psi) = \int_K \nabla \phi \cdot \nabla \psi,$$

and let $\Pi_K^\nabla : H^1(K) \rightarrow \mathbb{P}_m(K)$ denote the projection defined by

$$a^K(\Pi_K^\nabla \phi, p) = a^K(\phi, p), \quad \forall p \in \mathbb{P}_m, \quad \int_K \Pi_K^\nabla \phi = \int_K \phi.$$

We recall that for $w_h \in V^{K,m}$, $\Pi_K^\nabla w_h$ can be computed directly from the values of the degrees of freedom ([6]) without the need of explicitly constructing it (which would imply somehow solving a partial differential equation), by taking advantage of the identity

$$\int_K \nabla w_h \cdot \nabla p = - \int_K w_h \Delta p + \int_{\partial K} w_h \frac{\partial p}{\partial \nu_K},$$

that allows to express the term of the left hand side in terms of the interior moments of w_h (for $p \in \mathbb{P}_m$, Δp is a polynomial of degree less than or equal to $m - 2$) and of an integral on the boundary (where w_h is a known piecewise polynomial). Letting \mathbb{P}_m^* denote the space of discontinuous piecewise polynomials of order less than or equal to m

$$\mathbb{P}_m^* = \{\phi \in L^2(\Omega) : \phi|_K \in \mathbb{P}_m \ \forall K \in \mathcal{T}_h\},$$

we let $\Pi^\nabla : H^1(\Omega) \rightarrow \mathbb{P}_m^*$ be defined by assembling, element by element, the Π_K^∇ 's:

$$\Pi^\nabla \phi|_K = \Pi_K^\nabla(\phi|_K), \quad \forall K \in \mathcal{T}_h.$$

The discretization of (2.1) by the Nitsche's method would consist in looking for $u_h \in V_h$ such that for all $v_h \in V_h$ one has

$$a(u_h, v_h) - \int_{\partial\Omega} \partial_\nu u_h v_h - \int_{\partial\Omega} u_h \partial_\nu v_h + \gamma h^{-1} \int_{\partial\Omega} u_h v_h = \int_{\Omega} f v_h - \int_{\partial\Omega} g \partial_\nu v_h + \gamma h^{-1} \int_{\partial\Omega} g v_h,$$

where ∂_ν stands for $\partial/\partial\nu$, ν denoting the outer normal to Ω . As typical for the Virtual Element method, both at the right hand side and at the left hand side of such an equation we find terms which are not “computable”, that is that can not be computed exactly with only the knowledge of the value of the degrees of freedom of u_h and v_h . Besides the bilinear form a , which can be treated

by the standard approach, this is the case for all the terms involving $\partial_\nu u_h$ and $\partial_\nu v_h$. As usually done in VEM, the bilinear form a is then replaced with

$$a_h(u_h, v_h) = \sum_K a_h^K(u_h, v_h),$$

where

$$a_h^K(\phi, \psi) = a^K(\Pi_K^\nabla \phi, \Pi_K^\nabla \psi) + S_a^K(\phi - \Pi_K^\nabla \phi, \psi - \Pi_K^\nabla \psi).$$

We recall that different choices are possible for the bilinear form S_a^K (see [8]), the essential requirement being that it satisfies

$$a^K(\phi, \phi) \lesssim S_a^K(\phi, \phi) \lesssim a^K(\phi, \phi), \quad \forall \phi \in V^{K,m} \text{ with } \Pi_K^\nabla \phi = 0,$$

so that the local discrete bilinear forms satisfy the following two properties:

- *Stability:*

$$a^K(\phi, \phi) \lesssim a_h^K(\phi, \phi) \lesssim a^K(\phi, \phi), \quad \forall \phi \in V^{K,m}$$

- *m-consistency:* for any $\phi \in V_h$ and $p \in \mathbb{P}_m(K)$

$$(2.6) \quad a_h^K(\phi, p) = a^K(\phi, p).$$

In the numerical tests performed in Section 4 we made the standard choice of defining S_a^K in terms of the vectors of local degrees of freedom as the properly scaled euclidean scalar product.

As far as the terms involving the normal derivative are concerned, we treat them by replacing $\partial_\nu u_h$ and $\partial_\nu v_h$, boundary edge by boundary edge, respectively with $\partial_\nu \Pi^\nabla(u_h)$ and $\partial_\nu \Pi^\nabla(v_h)$. Then we can write the Nitsche's method for the VEM discretization of 3.1 as: find $u_h \in V_h$ such that for all $v_h \in V_h$ it holds that

$$(2.7) \quad a_h(u_h, v_h) - \sum_{e \in \mathcal{E}^\partial} \int_e \partial_\nu \Pi^\nabla(u_h) v_h - \sum_{e \in \mathcal{E}^\partial} \int_e \partial_\nu \Pi^\nabla(v_h) u_h + \gamma h^{-1} \int_{\partial\Omega} u_h v_h \\ = \int_\Omega f v_h - \sum_{e \in \mathcal{E}^\partial} \int_e g (\partial_\nu \Pi^\nabla(v_h) - \gamma h^{-1} v_h),$$

where γ is a positive constant and \mathcal{E}^∂ denotes the set of edges of \mathcal{T}_h lying on $\partial\Omega$.

We introduce the norm:

$$(2.8) \quad \|\phi\|_\Omega^2 = |\phi|_{1,\Omega}^2 + h^{-1} \|\phi\|_{0,\partial\Omega}^2$$

and the space $\mathcal{H}(\Omega)$ defined as the closure of $C^\infty(\Omega)$ with respect to the norm $\|\cdot\|_\Omega$. Setting

$$(2.9) \quad \mathcal{B}_{h,\gamma}(\phi, \psi) = a_h(\phi, \psi) - \sum_{e \in \mathcal{E}^\partial} \int_e \partial_\nu \Pi^\nabla(\phi) \psi - \sum_{e \in \mathcal{E}^\partial} \int_e \partial_\nu \Pi^\nabla(\psi) \phi + \gamma h^{-1} \int_{\partial\Omega} \phi \psi,$$

we start by proving the following lemma:

Lemma 2.2. *For all $\phi, \psi \in \mathcal{H}(\Omega)$ we have*

$$(2.10) \quad |\mathcal{B}_{h,\gamma}(\phi, \psi)| \lesssim \|\phi\|_\Omega \|\psi\|_\Omega.$$

Moreover, there exists $\gamma_0 > 0$ such that, for $\gamma > \gamma_0$, the bilinear form $\mathcal{B}_{h,\gamma}$ verifies for all $\phi \in V_h$

$$(2.11) \quad \mathcal{B}_{h,\gamma}(\phi, \phi) \gtrsim \|\phi\|_\Omega^2,$$

(the implicit constant in the two inequalities depending on γ).

Proof. We observe that, since $\Pi^\nabla(\phi)$ is a polynomial, it is not difficult to verify that the following inverse bound holds:

$$(2.12) \quad \|\partial_\nu \Pi^\nabla(\phi)\|_{0,e} \lesssim h^{-1/2} |\Pi^\nabla(\phi)|_{1,K_e} \lesssim h^{-1/2} |\phi|_{1,K_e},$$

where, for $e \in \mathcal{E}^\partial$, K_e is the unique polygon of the tessellation having e as an edge. Then we have

$$\sum_{e \in \mathcal{E}^\partial} \int_e \partial_\nu \Pi^\nabla(\phi) \psi \lesssim \sum_{e \in \mathcal{E}^\partial} \|\partial_\nu \Pi^\nabla(\phi)\|_{0,e} \|\psi\|_{0,e} \lesssim \sum_{e \in \mathcal{E}^\partial} |\phi|_{1,K_e} h^{-1/2} \|\psi\|_{0,e}.$$

Obtaining (2.10) is then not difficult. As far as (2.11) is concerned, we have

$$(2.13) \quad \mathcal{B}_{h,\gamma}(\phi, \phi) = a_h(\phi, \phi) + \gamma h^{-1} \|\phi\|_{0,\partial\Omega}^2 - 2 \langle \partial_\nu \Pi^\nabla(\phi), \phi \rangle$$

where we use the notation

$$\langle \phi, \psi \rangle = \sum_{e \in \mathcal{E}^\partial} \int_e \phi \psi.$$

We now have the following bounds

$$\langle \partial_\nu \Pi^\nabla(\phi), \phi \rangle \lesssim \sum_{e \in \mathcal{E}^\partial} \|\partial_\nu \Pi^\nabla(\phi)\|_{0,e} \|\phi\|_{0,e}$$

Thanks to the inverse inequality (2.12), we can write, for $\varepsilon > 0$ arbitrary,

$$\langle \partial_\nu \Pi^\nabla(\phi), \phi \rangle \lesssim \sum_{e \in \mathcal{E}^\partial} h^{-1/2} |\phi|_{1,K_e} \|\phi\|_{0,e} \lesssim \frac{\varepsilon}{2} |\phi|_{1,\Omega}^2 + \frac{1}{2\varepsilon} h^{-1} \|\phi\|_{0,\partial\Omega}^2.$$

Substituting into (2.13) we obtain, for a fixed positive constant c_1 independent of h

$$\mathcal{B}_{h,\gamma}(\phi, \phi) \gtrsim (1 - c_1 \varepsilon) |\phi|_{1,\Omega}^2 + (\gamma - \frac{c_1}{\varepsilon}) h^{-1} \|\phi\|_{0,\partial\Omega}^2.$$

We now choose $\varepsilon = 1/(2c_1)$ and if $\gamma > \gamma_0$ with γ_0 chosen in such a way that $\gamma_0 - c_1/\varepsilon > 0$, the thesis easily follows. \square

Existence and uniqueness of the solution of (2.7) easily follow.

We are then able to prove the following result:

Theorem 2.3. *If $u \in H^s(\Omega)$, with $2 \leq s \leq m+1$, and if we chose $\gamma > \gamma_0$, with γ_0 given by Lemma 2.2, then the following error estimate holds*

$$\|u - u_h\|_\Omega \lesssim h^{s-1} |u|_{s,\Omega}.$$

Proof. Let u_I denote the VEM interpolant and $u_\pi \in \mathbb{P}_m^*$ the $L^2(\Omega)$ projection of u onto the space of discontinuous piecewise polynomials. For any j, k with $0 \leq j \leq k \leq m+1$ we have, for $u \in L^2(\Omega)$ with $u|_K \in H^k(K)$

$$(2.14) \quad \|w - w_\pi\|_{j,K} \lesssim h_K^{k-j} |w|_{k,K}.$$

For $j \geq 1$ the bound (2.14) can be proven by a standard argument combining the bound for $j = 0$ with an inverse inequality. Moreover we have, for $e \in \mathcal{E}^K \cap \mathcal{E}^\partial$,

$$(2.15) \quad \|\partial_\nu(w - w_\pi)\|_{0,e} \lesssim h^{-1/2} |w - w_\pi|_{1,K} + h^{1/2} |w - w_\pi|_{2,K} \lesssim h^{s-3/2} |w|_{s,K}.$$

We set $d_h = u_I - u_h$. Using the definition (2.9), summing and subtracting u_π , using the m -consistency (2.6) to replace $a_h(u_\pi, d_h)$ with $a(u_\pi, d_h)$ and then, summing and subtracting u , we can write

$$\begin{aligned}
 (2.16) \quad \|u_I - u_h\|_\Omega^2 &\lesssim \mathcal{B}_{h,\gamma}(u_I, d_h) - \mathcal{B}_{h,\gamma}(u_h, d_h) = \\
 &= \sum_{K \in \mathcal{T}_h} a_h^K(u_I - u_\pi, d_h) + \sum_{K \in \mathcal{T}_h} a^K(u_\pi - u, d_h) + a(u, d_h) - \langle \partial_\nu u, d_h \rangle + \\
 &\quad \langle \partial_\nu(u - \Pi^\nabla(u_I)), d_h \rangle - \langle u, \partial_\nu \Pi^\nabla(d_h) \rangle + \langle u - u_I, \partial_\nu \Pi^\nabla(d_h) \rangle + \gamma h^{-1} \langle u, d_h \rangle \\
 &\quad + \gamma h^{-1} \langle u_I - u, d_h \rangle - \int_\Omega f d_h + \langle g, \partial_\nu \Pi^\nabla(d_h) - \gamma h^{-1} d_h \rangle \\
 &= E1 + E2 + E3 + E4 + E5.
 \end{aligned}$$

with

$$\begin{aligned}
 E1 &= \sum_{K \in \mathcal{T}_h} a_h^K(u_I - u_\pi, d_h), \quad E2 = \sum_{K \in \mathcal{T}_h} a^K(u_\pi - u, d_h), \quad E3 = \langle \partial_\nu(u - \Pi^\nabla(u_I)), d_h \rangle \\
 E4 &= \langle u - u_I, \partial_\nu \Pi^\nabla(d_h) \rangle, \quad E5 = \gamma h^{-1} \langle u_I - u, d_h \rangle,
 \end{aligned}$$

where we used that, as u is the solution of (2.1),

$$a(u, d_h) - \langle \partial_\nu u, d_h \rangle - \int_\Omega f d_h = 0, \quad \langle u, \partial_\nu \Pi^\nabla(d_h) \rangle - \gamma h^{-1} \langle u, d_h \rangle - \langle g, \partial_\nu \Pi^\nabla(d_h) - \gamma h^{-1} d_h \rangle = 0.$$

Let us then bound the different components of the error.

Both $E1$ and $E2$ are standardly encountered in the analysis of the VEM method, and a bound can be found in the literature (see e.g. [4]), yielding

$$E1 \lesssim |d_h|_{1,\Omega} h^{s-1} |u|_{s,\Omega}, \quad \text{and} \quad E2 \lesssim |d_h|_{1,\Omega} h^{s-1} |u|_{s,\Omega}.$$

On the other hand we have

$$E3 \lesssim \sum_{e \in \mathcal{E}^\partial} \|\partial_\nu(u - \Pi^\nabla(u_I))\|_{0,e} \|d_h\|_{0,e}.$$

Now, using (2.15), we have

$$\|\partial_\nu(u - \Pi^\nabla(u_I))\|_{0,e} \leq \|\partial_\nu(u - u_\pi)\|_{0,e} + \|\partial_\nu \Pi^\nabla(u_\pi - u_I)\|_{0,e} \lesssim h^{s-3/2} |u|_{s,K} + h^{-1/2} (|u_\pi - u_I|_{1,K} + |u_I - u|_{1,K})$$

yielding

$$E3 \lesssim h^{s-1} h^{-1/2} |u|_{s,\Omega} \|d_h\|_{0,\partial\Omega}.$$

As far as $E4$ is concerned we have

$$E4 \leq \sum_{e \in \mathcal{E}^\partial} \|u - u_I\|_{0,e} \|\partial_\nu \Pi^\nabla(d_h)\|_{0,e} \lesssim \sum_{e \in \mathcal{E}^\partial} h^{s-1/2} |u|_{s,K_e} h^{-1/2} |d_h|_{1,K_e} \lesssim h^{s-1} |u|_{s,\Omega} |d_h|_{1,\Omega}.$$

A similar argument yields

$$E5 \lesssim h^{s-1} |u|_{s,\Omega} h^{-1/2} \|d_h\|_{0,\partial\Omega},$$

finally giving

$$\|u_I - u_h\|_\Omega^2 \lesssim h^{s-1} |u|_{s,\Omega} \|u_I - u_h\|_\Omega.$$

Dividing both sides by $\|u_I - u_h\|_\Omega$ and using a triangular inequality we get the thesis. \square

3. THE VIRTUAL ELEMENT METHOD ON DOMAINS WITH CURVED BOUNDARY

Let now consider the solution of the same model problem

$$(3.1) \quad -\Delta u = f, \text{ in } \Omega, \quad u = g, \text{ on } \partial\Omega$$

with, once again, $f \in L^2(\Omega)$, $g \in H^{1/2}(\partial\Omega)$, where now $\Omega \subseteq \mathbb{R}^2$ is a convex domain with curved boundary $\partial\Omega$ assumed, for the sake of convenience, to be of class C^∞ . In order to solve such a problem by the Virtual Element method, we assume that Ω is approximated by a family of polygonal domains Ω_h , $0 < h \leq 1$, each endowed with a quasi uniform shape regular tessellation \mathcal{T}_h into polygons K with diameter $h_K \simeq h$. We assume that all the vertices of \mathcal{T}_h lying on $\partial\Omega_h$ also lie on $\partial\Omega$. As Ω is convex this implies that $\Omega_h \subseteq \Omega$.

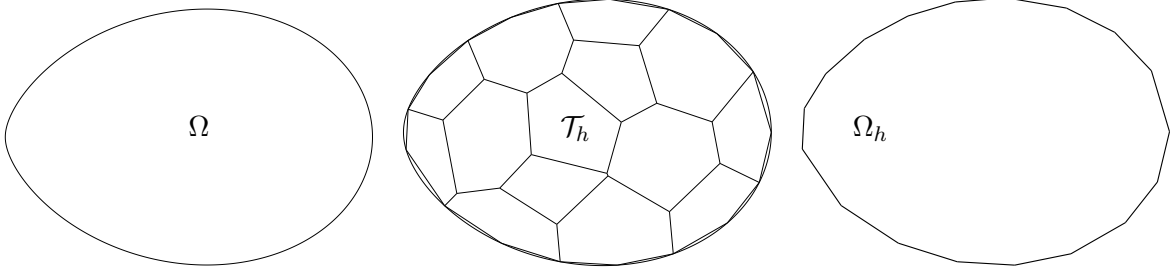


FIGURE 1. Domain Ω , tessellation \mathcal{T}_h of Ω into shape regular polygons and polygonal domain $\Omega_h \subseteq \Omega$ approximating Ω .

3.1. The Projection Method of Bramble, Dupont and Thomée. In order to deal with the curved boundary, following [14] we apply on the approximating domain Ω_h a modified version of Nitsche's method, which takes into account that the boundary data is given on $\partial\Omega$ rather than on $\partial\Omega_h$.

Letting ν_h be the outer normal to Ω_h , for $x \in \partial\Omega_h$ we let $\delta(x) > 0$ denote the non negative scalar such that

$$x + \delta(x)\nu_h(x) \in \partial\Omega.$$

It is known ([14]) that, as Ω is smooth and convex, we have that

$$(3.2) \quad \delta_h = \sup_{x \in \partial\Omega_h} \delta(x) = o(h^2).$$

We let $V_h \subset H^1(\Omega_h)$ be the order m VEM discretization space relative to the tessellation \mathcal{T}_h (defined by (2.4)). Setting $k = \lfloor m/2 \rfloor$, the projection method of [14] reads as follows: find $u_h \in V_h$ such that for all $v_h \in V_h$ it holds that

$$(3.3) \quad \mathcal{B}_{h,\gamma}(u_h, v_h) - \sum_{e \in \mathcal{E}^\partial} \int_e \left(\sum_{j=1}^k \frac{\delta^j}{j!} \partial_{\nu_h}^j \Pi^\nabla(u_h) \right) (\partial_{\nu_h} \Pi^\nabla(v_h) - \gamma h^{-1} v_h) \\ = \int_{\Omega_h} f v_h - \sum_{e \in \mathcal{E}^\partial} \int_e g^\star (\partial_{\nu_h} \Pi^\nabla v_h - \gamma h^{-1} v_h)$$

where $\partial_{\nu_h}^j u = (\partial_{\nu_h})^j u$ denotes the j -th partial derivative of u in the ν_h direction and where, for $x \in \partial\Omega_h$,

$$g^\star(x) = g(x + \delta(x)\nu_h(x)).$$

We then introduce the bilinear form $\mathcal{A}_{h,\gamma}$ defined by

$$(3.4) \quad \mathcal{A}_{h,\gamma}(\phi, \psi) = \mathcal{B}_{h,\gamma}(\phi, \psi) - \sum_{e \in \mathcal{E}^\partial} \int_e \left(\sum_{j=1}^k \frac{\delta_h^j}{j!} \partial_{\nu_h}^j \Pi^\nabla(u_h) \right) (\partial_{\nu_h} \Pi^\nabla(v_h) - \gamma h^{-1} v_h),$$

and prove the following lemma:

Lemma 3.1. *For all ϕ, ψ in $\mathcal{H}(\Omega_h)$ it holds that*

$$(3.5) \quad |\mathcal{A}_{h,\gamma}(\phi, \psi)| \lesssim \|\phi\|_{\Omega_h} \|\psi\|_{\Omega_h}.$$

Moreover, there exists $\gamma_0 > 0$ such that for all $\gamma > 0$ the bilinear form $\mathcal{A}_{h,\gamma}$ verifies for all $\phi \in V_h$

$$(3.6) \quad \mathcal{A}_{h,\gamma}(\phi, \phi) \gtrsim \|\phi\|_{\Omega_h}^2$$

provided $h < h_0$ with $h_0 = h_0(\gamma) > 0$.

Proof. Let \mathcal{C}_k be defined as

$$\mathcal{C}_k(\phi, \psi) = \sum_{e \in \mathcal{E}^\partial} \int_e \left(\sum_{j=1}^k \frac{\delta_h^j}{j!} \partial_{\nu_h}^j \phi \right) \psi$$

so that we can write

$$\mathcal{A}_{h,\gamma}(\phi, \phi) = \mathcal{B}_{h,\gamma}(\phi, \psi) - \mathcal{C}_k(\Pi^\nabla(\phi), \partial_{\nu_h} \Pi^\nabla(\psi) - \gamma h^{-1} \psi).$$

As for all $\phi \in H^1(K)$, $\Pi_K^\nabla(\phi)$ is a piecewise polynomial, using an inverse inequality and the continuity of the operator Π_K^∇ we get that for $e \in \mathcal{E}^\partial$ and $\phi \in H^1(\Omega)$ we have

$$(3.7) \quad \|\partial_{\nu_h}^j \Pi_K^\nabla(\phi)\|_{0,e} \lesssim h^{1/2-j} |\Pi_K^\nabla(\phi)|_{1,K_e} \lesssim h^{1/2-j} |\phi|_{1,K_e},$$

where, once again, K_e is the unique element of \mathcal{T}_h having e as an edge. Since $\delta_h/h \lesssim 1$, using (3.7) we have

$$(3.8) \quad |\mathcal{C}_k(\Pi^\nabla(\phi), \psi)| \lesssim \sum_{e \in \mathcal{E}^\partial} \sum_{j=1}^k \left(\frac{\delta_h}{h} \right)^j h^j \|\partial_{\nu_h}^j \Pi^\nabla(\phi)\|_{0,e} \|\psi\|_{0,e} \lesssim \frac{\delta_h}{h} |\phi|_{1,\Omega_h} h^{1/2} \|\psi\|_{0,e}$$

as well as

$$(3.9) \quad |\mathcal{C}_k(\Pi^\nabla(\phi), \partial_{\nu_h} \Pi^\nabla(\psi))| \lesssim \sum_{e \in \mathcal{E}^\partial} \sum_{j=1}^k \left(\frac{\delta_h}{h} \right)^j h^j \|\partial_{\nu_h}^j \Pi^\nabla(\phi)\|_{0,e} \|\partial_{\nu_h} \Pi^\nabla(\psi)\|_{0,e} \lesssim \frac{\delta_h}{h} |\phi|_{1,\Omega_h} |\psi|_{1,\Omega_h}.$$

Combining with (2.10) the bound (3.5) easily follows. Let us now consider (3.6). Combining (2.11) with (3.8) and (3.9) we obtain, for $\varepsilon > 0$ arbitrary and c_1, c_2 and c_3 fixed positive constants,

$$\begin{aligned} \mathcal{A}_{h,\gamma}(\phi, \phi) &= \mathcal{B}_{h,\gamma}(\phi, \phi) - \mathcal{C}_k(\Pi^\nabla(\phi), \partial_{\nu_h} \Pi^\nabla(\phi)) + \gamma h^{-1} \mathcal{C}_k(\Pi^\nabla(\phi), \phi) \\ &\gtrsim (1 - c_1 \varepsilon - c_2 \frac{\delta_h}{h} - c_3 \frac{\delta_h}{h} \gamma) |\phi|_{1,\Omega_h}^2 + (\gamma - \frac{c_1}{\varepsilon} - c_3 \gamma \frac{\delta_h}{h}) h^{-1} \|\phi\|_{0,\partial\Omega_h}^2. \end{aligned}$$

We now choose $\varepsilon = 1/(2c_1)$ and we fix γ_0 in such a way that $\gamma_0 - c_1/\varepsilon > 0$. For $\gamma > \gamma_0$, set now $\alpha = \gamma - c_1/\varepsilon > 0$. As $\delta_h = o(h^2)$, we can choose h_0 in such a way that for all $h < h_0$, $c_2 \delta_h/h + \gamma c_3 \delta_h/h < 1/2$ and $\gamma c_3 \delta_h/h < \alpha$. The thesis easily follows. \square

Once again, existence and uniqueness of the solution of (3.3) easily follow. Moreover, the error estimate given by the following Theorem hold.

Theorem 3.2. *If $u \in H^s(\Omega) \cap W^{k+1,\infty}(\Omega)$, with $k+1 < s \leq m+1$, for $h < h_0$ and $\gamma > \gamma_0$ ($\gamma > 0$ and $h_0 > 0$ given by Lemma 3.1) the following error estimate holds*

$$\|u - u_h\|_{\Omega_h} \lesssim h^{s-1} |u|_{s,\Omega} + h^{-1/2} \delta^{k+1} \|u\|_{k+1,\infty,\Omega}.$$

Proof. Let u_I denote the usual VEM interpolant. Setting $d_h = u_I - u_h$ and proceeding as in Theorem 2.3, we have

$$\begin{aligned}
 (3.10) \quad \|u_I - u_h\|_{\Omega_h}^2 &\lesssim \mathcal{A}_{h,\gamma}(u_I, d_h) - \mathcal{A}_{h,\gamma}(u_h, d_h) = \\
 &\sum_{K \in \mathcal{T}_h} a_h^K(u_I - u_\pi, d_h) + \sum_K a^K(u_\pi - u, d_h) + a(u, d_h) - \langle \partial_{\nu_h} u, d_h \rangle + \\
 &\langle \partial_{\nu_h}(u - \Pi^\nabla(u_I)), d_h \rangle - \langle u, \partial_{\nu_h} \Pi^\nabla(d_h) \rangle + \langle u - u_I, \partial_{\nu_h} \Pi^\nabla(d_h) \rangle + \gamma h^{-1} \langle u, d_h \rangle \\
 &+ \gamma h^{-1} \langle u_I - u, d_h \rangle - \mathcal{C}_k(u, \partial_{\nu_h} \Pi^\nabla(d_h) - \gamma h^{-1} d_h) + \mathcal{C}_k(u - \Pi^\nabla(u_I), \partial_{\nu_h} \Pi^\nabla(d_h) - \gamma h^{-1} d_h) \\
 &- \int_{\Omega_h} f d_h + \langle g^\star, \partial_{\nu_h} \Pi^\nabla(d_h) - \gamma h^{-1} d_h \rangle \\
 &= E1 + E2 + E3 + E4 + E5 + E6 + E7.
 \end{aligned}$$

with $E1, E2, E3, E4$, and $E5$ as in the proof of Theorem 2.3 and with

$$E6 = \mathcal{C}_k(u - \Pi^\nabla(u_I), \partial_{\nu_h} \Pi^\nabla(d_h)) - \gamma h^{-1} d_h, \quad E7 = \langle g^\star - \sum_{j=0}^k \frac{\delta^j}{j!} \partial_{\nu_h}^j u, \partial_{\nu_h} \Pi^\nabla(d_h) - \gamma h^{-1} d_h \rangle.$$

The components $E1, E2, E3, E4, E5$ can be bounded exactly as in Theorem 2.3. Let us then bound the last two terms $E6$ and $E7$. Since $\delta = o(h^2) \lesssim h$, we have

$$E6 \lesssim \sum_{e \in \mathcal{E}^\partial} \sum_{j=1}^k h^j \|\partial_{\nu_h}^j (u - \Pi^\nabla(u_I))\|_{0,e} (\|\partial_{\nu_h} \Pi^\nabla(d_h)\|_{0,e} + h^{-1} \|d_h\|_{0,e}).$$

Now, using (2.3) as well as (3.7) we have

$$\begin{aligned}
 \|\partial_{\nu_h}^j (u - \Pi^\nabla(u_I))\|_{0,e} &\lesssim \|\partial_{\nu_h}^j (u - u_\pi)\|_{0,e} + \|\partial_{\nu_h}^j (\Pi^\nabla(u_\pi - u_I))\|_{0,e} \\
 &\lesssim h^{-1/2} |u - u_\pi|_{j, K_e} + h^{1/2} |u - u_\pi|_{j+1, K_e} + h^{1/2-j} |u_\pi - u_I|_{1, K_e} \lesssim h^{s-j-1/2} |u|_{s, K_e},
 \end{aligned}$$

where $|u_\pi - u_I|_{1, K_e}$ is bound by adding and subtracting u and using the VEM approximation bounds (2.5) and (2.14), yielding

$$E6 \lesssim h^{s-1} |u|_{s, \Omega} \|d_h\|_{\Omega_h}.$$

Finally, $E7$ takes into account the approximation of the curved boundary by projection, and, following the paper by Thomée, it can be bound as

$$E7 \lesssim \sum_{e \in \mathcal{E}^\partial} \|g^\star - \sum_{j=0}^k \frac{\delta^j}{j!} \partial_{\nu_h}^j u\|_{0,e} (\|\partial_{\nu_h} \Pi^\nabla(d_h)\|_{0,e} + h^{-1} \|d_h\|_{0,e}) \lesssim h^{-1/2} \delta^{k+1} \|u\|_{k+1, \infty, \Omega_h} \|d_h\|_{\Omega_h}.$$

Assembling the bounds for the seven terms we finally obtain

$$\|d_h\|_{\Omega_h}^2 \lesssim h^{s-1} |u|_{s, \Omega_h} \|\delta_h\|_{\Omega_h} + h^{-1/2} \delta^{k+1} \|u\|_{k+1, \infty, \Omega} \|\delta_h\|_{\Omega_h}.$$

Dividing both sides by $\|d_h\|_{\Omega_h}$ and using a triangular inequality we get the thesis. \square

As $\delta = d(h^2)$ and since we set $k = \lfloor m/2 \rfloor$ so that $h^{-1/2} \delta^{k+1} \lesssim h^{2\lfloor m/2 \rfloor + 3/2} \lesssim h^m$ we have the following corollary.

Corollary 3.3. *Under the assumptions of Theorem 3.2, if $u \in H^{m+1}(\Omega)$ then*

$$\|u - u_h\|_{\Omega_h} \lesssim h^m \|u\|_{m+1, \Omega}.$$

Remark 3.4. While, for the sake of simplicity, we assumed Ω to be convex, our reasoning can be carried out to more general situations, provided $d_h = o(h)$. In particular, for non convex domains, Theorem 3.2 holds, provided $\Omega_h \subseteq \Omega$ (which, if Ω is not convex, requires to give up the assumption that the boundary vertices of \mathcal{T}_h belong to $\partial\Omega$). For an extension of the method where this assumption is relaxed, see [16].

Remark 3.5. In defining the method, we set $k = \lfloor m/2 \rfloor$. Of course, it is possible to choose other values for the parameter k (for instance, if the condition $d_h = o(h^2)$ is not satisfied). Observe that, in the finite element case, the choice $k = m$ leads to the following discrete equation:

$$a(u_h, v_h) - \int_{\partial\Omega_h} \partial_{\nu_h} u_h v_h - \int_{\partial\Omega_h} u_h^* (\partial_{\nu_h} v_h - \gamma h^{-1} v_h) = \int_{\Omega} f v_h - \int_{\partial\Omega_h} g^* (\partial_{\nu_h} v_h - \gamma h^{-1} v_h)$$

where, for $x \in e \subset \Omega_h$, $u_h^*(x) = p(x + \delta(x)\nu_h(x))$, p being the polynomial in \mathbb{P}_m such that $u_h = p$ in K_e (K_e denoting the only triangular element having e as an edge). In our case we could expect that a similar property holds where p is replaced by $\Pi^\nabla(u_h)$. However, this is not the case (at least, not exactly). In fact, for $k = m$, if we rewrite (3.3) in such a way to single out $\Pi^\nabla(u_h)^*(x) = \Pi_{K_e}^\nabla(u_h)(x + \delta(x)\nu_h(x))$ we get

$$\begin{aligned} a_h(u_h, v_h) - \langle \partial_{\nu_h} \Pi^\nabla(u_h), v_h \rangle \\ - \langle \Pi^\nabla(u_h)^*, \partial_{\nu} \Pi^\nabla(v_h) - \gamma h^{-1} v_h \rangle + \langle \Pi^\nabla(u_h) - u_h, \partial_{\nu} \Pi^\nabla(v_h) - \gamma h^{-1} v_h \rangle \\ = \int_{\Omega_h} f v_h - \langle g^*, \partial_{\nu} \Pi^\nabla(v_h) - \gamma h^{-1} v_h \rangle, \end{aligned}$$

which contains an extra term measuring the discrepancy between u_h and $\Pi^\nabla(u_h)$ on $\partial\Omega_h$.

4. NUMERICAL TESTS

In this section we present three different sets of numerical experiments, aimed at testing and validating the proposed virtual element method for curved domains. More precisely we deal with the following three different test cases, for each of which the right hand side f and the boundary data g are chosen in such a way that the solution to our model problem is the one given by, respectively, (4.1), (4.2) and (4.3).

Test 1. $\Omega = \{(x, y) \in \mathbb{R}^2 | x^2 + y^2 \leq 1\}$. The analytic solution is given by

$$(4.1) \quad u(x, y) = \cos(4\pi\sqrt{x^2 + y^2}).$$

Test 2. Ω is the region bounded by the polar curve $x(\theta) = r(\theta)\cos(\theta)$, $y(\theta) = r(\theta)\sin(\theta)$, with $r(\theta) = 2 + \sin(9\theta)$, $\theta \in [0, 2\pi]$. The analytic solution is given by

$$(4.2) \quad u(x, y) = \text{sinc}(2.25\sqrt{x^2 + y^2}) \cos(6.75\pi\sqrt{x^2 + y^2}).$$

Test 3. Ω is the region bounded by the following curves:

$$\begin{aligned} x(\theta) &= r(\theta)\cos(\theta), \quad y(\theta) = r(\theta)\sin(\theta), \quad \text{with } r(\theta) = \sqrt{\theta}, \quad \theta \in [\pi/2, 8\pi], \\ x(\theta) &= r(\theta)\cos(\theta), \quad y(\theta) = r(\theta)\sin(\theta), \quad \text{with } r(\theta) = 0.9\sqrt{\theta}, \quad \theta \in [\pi/2, 8\pi], \\ \{0\} \times [0.9\sqrt{\pi/2}, \sqrt{\pi/2}], [0.9\sqrt{8\pi}, \sqrt{8\pi}] \times \{0\}. \end{aligned}$$

The analytic solution is given by

$$(4.3) \quad u(x, y) = \frac{\sin(32 \tan^{-1}(y/x)) \cos(96 \tan^{-1}(y/x))}{\sqrt{x^2 + y^2}}.$$

Figures 2, 3 and 4 display the three different domains considered (left) and the computed VEM solution for $m = 1$ (right).

Observe that, while the first of the three test cases falls under the assumptions under which we proved our theoretical estimate, this is not the case for the second and third test cases, for both of which the domain Ω is not convex. In all three cases, the tessellations \mathcal{T}_h consist in quasi uniform shape regular Voronoi decompositions of the domain considered. As the grids are not structured, we choose to define the mesh size parameter as $h = N_V^{-1/2}$, where N_V is the number of vertices of the tessellation.

Letting u_h^m denote the discrete solution obtained by the order m VEM method proposed in the previous section, for all the three tests we consider the relative error in the energy norm, as well as in the $L^2(\Omega_h)$ norm

$$(4.4) \quad e_m^S := \frac{\|u - u_h^m\|_{\Omega_h}}{\|u\|_{\Omega_h}}, \quad e_m^{L^2} := \frac{\|u - u_h^m\|_{0,\Omega_h}}{\|u\|_{0,\Omega_h}}.$$

Tables 1, 2 and 3 report e_m^S for the three test cases, for $m = [1, \dots, 6]$. We also display in Figures 5, 6, 7 a logarithmic plot of the energy norm error e_m^S and the L^2 norm $e_m^{L^2}$ as a function of the number of degrees of freedom N_{DoFs} (which, we recall, is asymptotically proportional to N_V). The plots also show the approximate asymptotic convergence estimate obtained by plotting the functions $N_{\text{DoFs}}^{-m/2} \simeq h^m$.

The numerical results for Test 1 are in agreement with the theoretical estimates. To test the robustness of the method we considered, in Tests 2 and 3, domains which are not convex; nevertheless the numerical results are also in agreement with the theory and the predicted convergence rate of Corollary 3.3 is attained, see Tables 3, 2 and Figures 7 and 6.

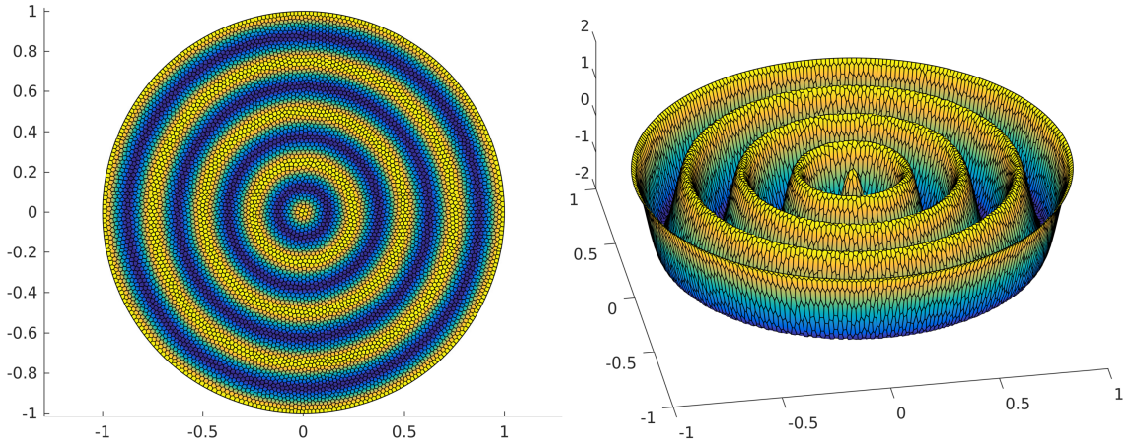


FIGURE 2. First test case: (left) example mesh; (right) solution computed on the example mesh for $m = 1$.

REFERENCES

1. P. F. Antonietti, L. Beirão da Veiga, D. Mora, and M. Verani, *A stream virtual element formulation of the Stokes problem on polygonal meshes*, SIAM Journal on Numerical Analysis **52** (2014), no. 1, 386–404.

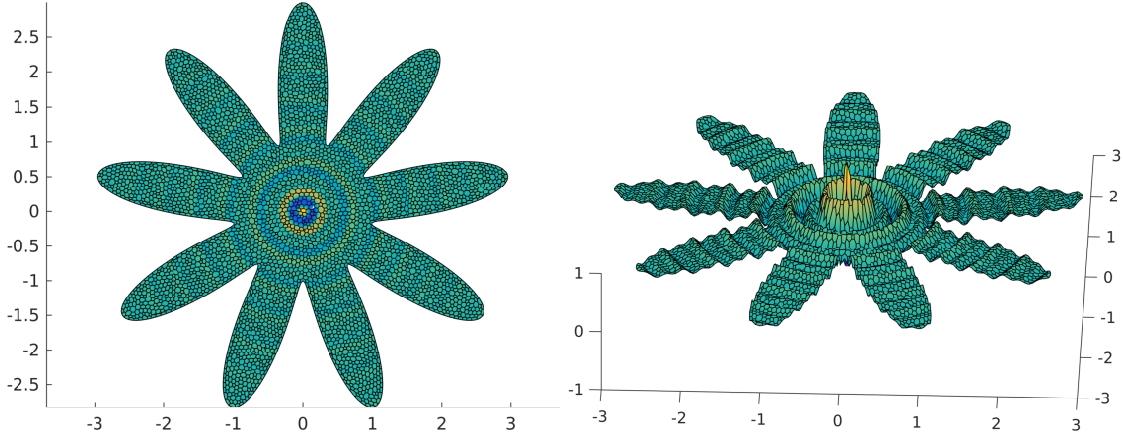


FIGURE 3. Second test case: (left) example mesh; (right) solution computed on the example mesh for $m = 1$.

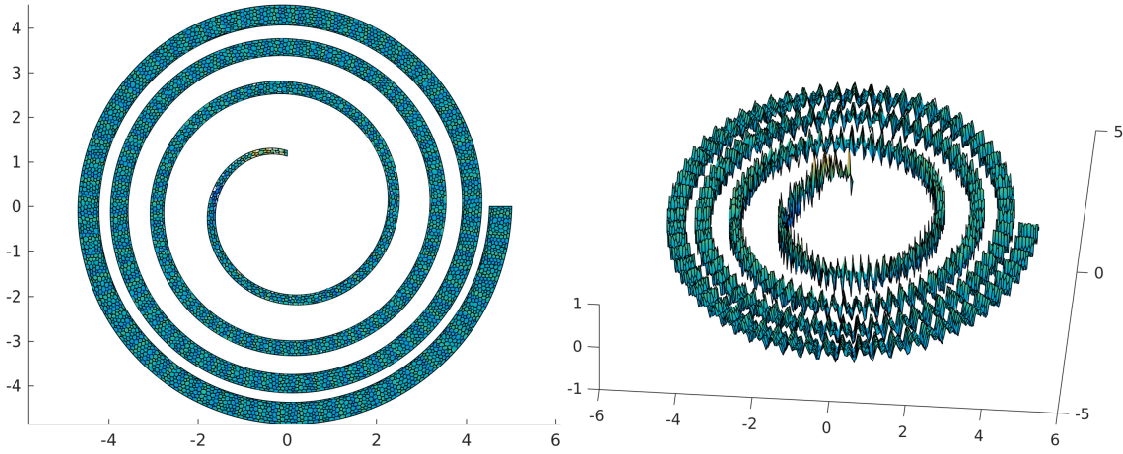


FIGURE 4. Third test case: (left) example mesh; (right) solution computed on the example mesh for $m = 1$.

2. P. F. Antonietti, L. Beirão da Veiga, S. Scacchi, and M. Verani, *A C^1 virtual element method for the Cahn-Hilliard equation with polygonal meshes*, SIAM Journal on Numerical Analysis **54** (2016), no. 1, 34–56.
3. P. F. Antonietti, L. Mascotto, and M. Verani, *A multigrid algorithm for the p -version of the virtual element method*, Math. Model. Numer. Anal. **52** (2018), no. 1, 337–364.
4. L. Beirão da Veiga, F. Brezzi, A. Cangiani, G. Manzini, L. D. Marini, and A. Russo, *Basic principles of virtual element methods*, Mathematical Models and Methods in Applied Sciences **23** (2013), no. 1, 199–214.
5. L. Beirão da Veiga, F. Brezzi, and L. Marini, *Virtual elements for linear elasticity problems*, SIAM Journal on Numerical Analysis **51** (2013), no. 2, 794–812.
6. L. Beirão da Veiga, F. Brezzi, L. D. Marini, and A. Russo, *The Hitchhiker's guide to the virtual element method*, Mathematical Models and Methods in Applied Sciences **24** (2014), no. 8, 1541–1573.
7. ———, *Mixed virtual element methods for general second order elliptic problems on polygonal meshes*, ESAIM: M2AN **50** (2016), no. 3, 727–747.
8. L. Beirão da Veiga, Lovadina C., and A. Russo, *Stability Analysis for the Virtual Element Method*, 2016, arXiv:1607.05988.
9. L. Beirão da Veiga, A. Chernov, L. Mascotto, and A. Russo, *Basic principles of hp virtual elements on quasiuniform meshes*, Mathematical Models and Methods in Applied Sciences **26** (2016), no. 8, 1567–1598.

TABLE 1. First test case: relative errors in the energy norm for $m = 1, \dots, 6$.

Mesh	h	e_1^S	e_2^S	e_3^S	e_4^S	e_5^S	e_6^S
u-circle ₁	$4.43 \cdot 10^{-2}$	$5.55 \cdot 10^{-2}$	$2.19 \cdot 10^{-2}$	$1.20 \cdot 10^{-2}$	$5.04 \cdot 10^{-3}$	$7.51 \cdot 10^{-4}$	$1.79 \cdot 10^{-4}$
u-circle ₂	$3.14 \cdot 10^{-2}$	$3.60 \cdot 10^{-2}$	$9.93 \cdot 10^{-3}$	$2.99 \cdot 10^{-3}$	$1.36 \cdot 10^{-3}$	$1.51 \cdot 10^{-4}$	$2.20 \cdot 10^{-5}$
u-circle ₃	$2.22 \cdot 10^{-2}$	$2.09 \cdot 10^{-2}$	$3.92 \cdot 10^{-3}$	$7.73 \cdot 10^{-4}$	$3.16 \cdot 10^{-4}$	$2.34 \cdot 10^{-5}$	$2.40 \cdot 10^{-6}$
u-circle ₄	$1.57 \cdot 10^{-2}$	$1.16 \cdot 10^{-2}$	$1.56 \cdot 10^{-3}$	$2.16 \cdot 10^{-4}$	$7.73 \cdot 10^{-5}$	$3.92 \cdot 10^{-6}$	$2.75 \cdot 10^{-7}$
u-circle ₅	$1.11 \cdot 10^{-2}$	$6.35 \cdot 10^{-3}$	$6.03 \cdot 10^{-4}$	$5.49 \cdot 10^{-5}$	$1.59 \cdot 10^{-5}$	$5.86 \cdot 10^{-7}$	$2.96 \cdot 10^{-8}$
u-circle ₆	$7.83 \cdot 10^{-3}$	$3.51 \cdot 10^{-3}$	$2.41 \cdot 10^{-4}$	$1.55 \cdot 10^{-5}$	$3.45 \cdot 10^{-6}$	$8.88 \cdot 10^{-8}$	$3.17 \cdot 10^{-9}$
u-circle ₇	$5.54 \cdot 10^{-3}$	$2.02 \cdot 10^{-3}$	$9.82 \cdot 10^{-5}$	$4.34 \cdot 10^{-6}$	$7.43 \cdot 10^{-7}$	$1.35 \cdot 10^{-8}$	$3.40 \cdot 10^{-10}$
u-circle ₈	$3.91 \cdot 10^{-3}$	$1.15 \cdot 10^{-3}$	$4.01 \cdot 10^{-5}$	$1.21 \cdot 10^{-6}$	$1.54 \cdot 10^{-7}$	$2.00 \cdot 10^{-9}$	$3.53 \cdot 10^{-11}$

TABLE 2. Second test case: relative errors in the energy norm for $m = 1, \dots, 6$.

Mesh	h	e_1^S	e_2^S	e_3^S	e_4^S	e_5^S	e_6^S
flower ₁	$1.40 \cdot 10^{-2}$	$5.50 \cdot 10^{-2}$	$3.02 \cdot 10^{-2}$	$1.07 \cdot 10^{-2}$	$4.72 \cdot 10^{-3}$	$9.85 \cdot 10^{-4}$	$2.02 \cdot 10^{-4}$
flower ₂	$1.01 \cdot 10^{-2}$	$3.40 \cdot 10^{-2}$	$1.29 \cdot 10^{-2}$	$2.95 \cdot 10^{-3}$	$1.20 \cdot 10^{-3}$	$1.33 \cdot 10^{-4}$	$2.39 \cdot 10^{-5}$
flower ₃	$7.26 \cdot 10^{-3}$	$1.94 \cdot 10^{-2}$	$6.02 \cdot 10^{-3}$	$8.59 \cdot 10^{-4}$	$3.15 \cdot 10^{-4}$	$2.21 \cdot 10^{-5}$	$4.13 \cdot 10^{-6}$
flower ₄	$5.19 \cdot 10^{-3}$	$1.24 \cdot 10^{-2}$	$2.53 \cdot 10^{-3}$	$2.57 \cdot 10^{-4}$	$7.08 \cdot 10^{-5}$	$3.64 \cdot 10^{-6}$	$3.79 \cdot 10^{-7}$
flower ₅	$3.70 \cdot 10^{-3}$	$7.16 \cdot 10^{-3}$	$1.12 \cdot 10^{-3}$	$7.64 \cdot 10^{-5}$	$1.66 \cdot 10^{-5}$	$5.83 \cdot 10^{-7}$	$4.56 \cdot 10^{-8}$
flower ₆	$2.63 \cdot 10^{-3}$	$4.27 \cdot 10^{-3}$	$4.71 \cdot 10^{-4}$	$2.37 \cdot 10^{-5}$	$3.64 \cdot 10^{-6}$	$9.02 \cdot 10^{-8}$	$4.83 \cdot 10^{-9}$
flower ₇	$1.87 \cdot 10^{-3}$	$2.65 \cdot 10^{-3}$	$2.02 \cdot 10^{-4}$	$7.11 \cdot 10^{-6}$	$7.86 \cdot 10^{-7}$	$1.38 \cdot 10^{-8}$	$5.60 \cdot 10^{-10}$

TABLE 3. Third test case: relative errors in the energy norm for $m = 1, \dots, 6$.

Mesh	h	e_1^S	e_2^S	e_3^S	e_4^S	e_5^S	e_6^S
spiral ₁	$1.23 \cdot 10^{-2}$	$2.13 \cdot 10^{-1}$	$1.95 \cdot 10^{-1}$	$1.95 \cdot 10^{-1}$	$1.54 \cdot 10^{-1}$	$1.58 \cdot 10^{-1}$	$1.43 \cdot 10^{-1}$
spiral ₂	$9.05 \cdot 10^{-3}$	$1.73 \cdot 10^{-1}$	$1.21 \cdot 10^{-1}$	$1.06 \cdot 10^{-1}$	$9.21 \cdot 10^{-2}$	$9.25 \cdot 10^{-2}$	$7.94 \cdot 10^{-2}$
spiral ₃	$6.63 \cdot 10^{-3}$	$9.40 \cdot 10^{-2}$	$5.74 \cdot 10^{-2}$	$4.91 \cdot 10^{-2}$	$3.55 \cdot 10^{-2}$	$2.41 \cdot 10^{-2}$	$1.59 \cdot 10^{-2}$
spiral ₄	$4.83 \cdot 10^{-3}$	$5.03 \cdot 10^{-2}$	$2.65 \cdot 10^{-2}$	$2.05 \cdot 10^{-2}$	$1.18 \cdot 10^{-2}$	$5.09 \cdot 10^{-3}$	$2.25 \cdot 10^{-3}$
spiral ₅	$3.48 \cdot 10^{-3}$	$2.30 \cdot 10^{-2}$	$1.42 \cdot 10^{-2}$	$6.38 \cdot 10^{-3}$	$2.96 \cdot 10^{-3}$	$7.50 \cdot 10^{-4}$	$2.87 \cdot 10^{-4}$
spiral ₆	$2.50 \cdot 10^{-3}$	$1.20 \cdot 10^{-2}$	$6.21 \cdot 10^{-3}$	$1.78 \cdot 10^{-3}$	$7.17 \cdot 10^{-4}$	$1.19 \cdot 10^{-4}$	$3.20 \cdot 10^{-5}$
spiral ₇	$1.79 \cdot 10^{-3}$	$6.81 \cdot 10^{-3}$	$2.54 \cdot 10^{-3}$	$4.73 \cdot 10^{-4}$	$1.57 \cdot 10^{-4}$	$1.57 \cdot 10^{-5}$	$3.08 \cdot 10^{-6}$

10. L. Beirão da Veiga, C. Lovadina, and G. Vacca, *Divergence free virtual elements for the Stokes problem on polygonal meshes*, ESAIM: M2AN **51** (2017), no. 2, 509–535.
11. ———, *Virtual Elements for the Navier-Stokes problem on polygonal meshes*, arXiv e-prints (2017).
12. L. Beirão da Veiga, A. Russo, and G. Vacca, *The Virtual Element Method with curved edges*, ArXiv e-prints (2017).
13. M. F. Benedetto, S. Berrone, and S. Scialó, *A globally conforming method for solving flow in discrete fracture networks using the virtual element method*, Finite Elements in Analysis and Design **109** (2016), 23 – 36.
14. J. H. Bramble, T. Dupont, and V. Thome, *Projection methods for dirichlet's problem in approximating polygonal domains with boundary-value corrections*, Mathematics of Computation **26** (1972), no. 120, 869–879.
15. L. Beirão da Veiga, C. Lovadina, and D. Mora, *A virtual element method for elastic and inelastic problems on polytope meshes*, Computer Methods in Applied Mechanics and Engineering **295** (2015), 327 – 346.
16. T. Dupont, *L_2 error estimates for projection methods for parabolic equations in approximating domains*, Mathematical Aspects of Finite Elements in Partial Differential Equations (Carl de Boor, ed.).
17. Brezzi F., Lipnikov K., and Shashkov M., *Convergence of mimetic finite difference method for diffusion problems on polyhedral meshes with curved faces*, Math. Models Methods Appl. Sci. **16** (2006), no. 2, 275–297.

18. M. Frittelli and I. Sgura, *Virtual Element Method for the Laplace-Beltrami equation on surfaces*, arXiv e-prints (2016).
19. A. L. Gain, C. Talischi, and G. H. Paulino, *On the virtual element method for three-dimensional linear elasticity problems on arbitrary polyhedral meshes*, Computer Methods in Applied Mechanics and Engineering **282** (2014), 132–160.
20. Botti L. and Di Pietro D., *Assessment of hybrid high-order methods on curved meshes and comparison with discontinuous galerkin methods*, J. Comput. Phys. **370** (2018), 58–84.
21. K. Lipnikov, *On shape-regularity of polyhedral meshes for solving pdes*.
22. L. Mascotto, L. Beirão da Veiga, A. Chernov, and A. Russo, *Exponential convergence of the hp Virtual Element Method with corner singularities*, Numer. Math. (2018), 138–581.
23. J.A. Nitsche, *Über ein variationsprinzip zur Lösung von Dirichlet-Problemen bei Verwendung von Teilräumen, die keinen Randbedingungen unterworfen sind*, Abhandlungen aus dem Mathematischen Seminar der Universität Hamburg **36** (1970), 9–15.
24. I. Perugia, P. Pietra, and A. Russo, *A plane wave virtual element method for the Helmholtz problem*, ESAIM: M2AN **50** (2016), no. 3, 783–808.
25. Sevilla R., Fernández-Méndez S., and Huerta A., *Comparison of high-order curved finite elements*, Internat. J. Numer. Methods Engrg. **87** (2011), no. 8, 719–734.
26. Vidar Thomée, *Polygonal domain approximation in dirichlet's problem*, IMA Journal of Applied Mathematics **11** (1973), no. 1, 33–44.
27. G. Vacca and L. Beirão da Veiga, *Virtual element methods for parabolic problems on polygonal meshes*, Numerical Methods for Partial Differential Equations **31** (2015), no. 6, 2110–2134.

IMATI “E. MAGENES”, CNR, PAVIA (ITALY)
E-mail address: `silvia.bertoluzza@imati.cnr.it`

IMATI “E. MAGENES”, CNR, PAVIA (ITALY)
E-mail address: `micol.pennacchio@imati.cnr.it`

IMATI “E. MAGENES”, CNR, PAVIA (ITALY)
E-mail address: `daniele.prada@imati.cnr.it`

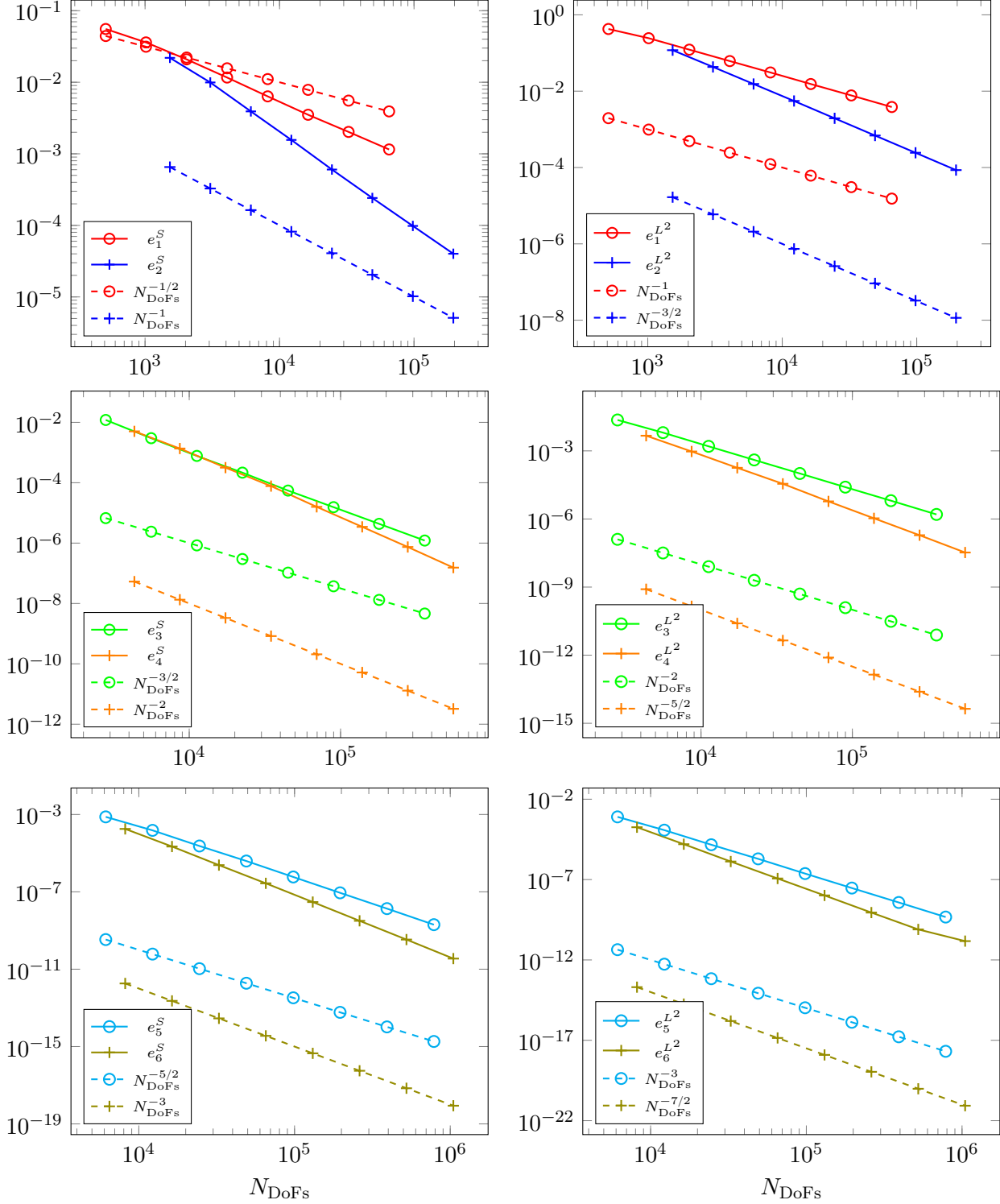


FIGURE 5. First test case: logary logarithmic plot of the energy norm error e_m^S for increasing polynomial order $m = 1, \dots, 6$ and of the functions $N_{\text{DoFs}}^{-m/2}$ (dashed lines).

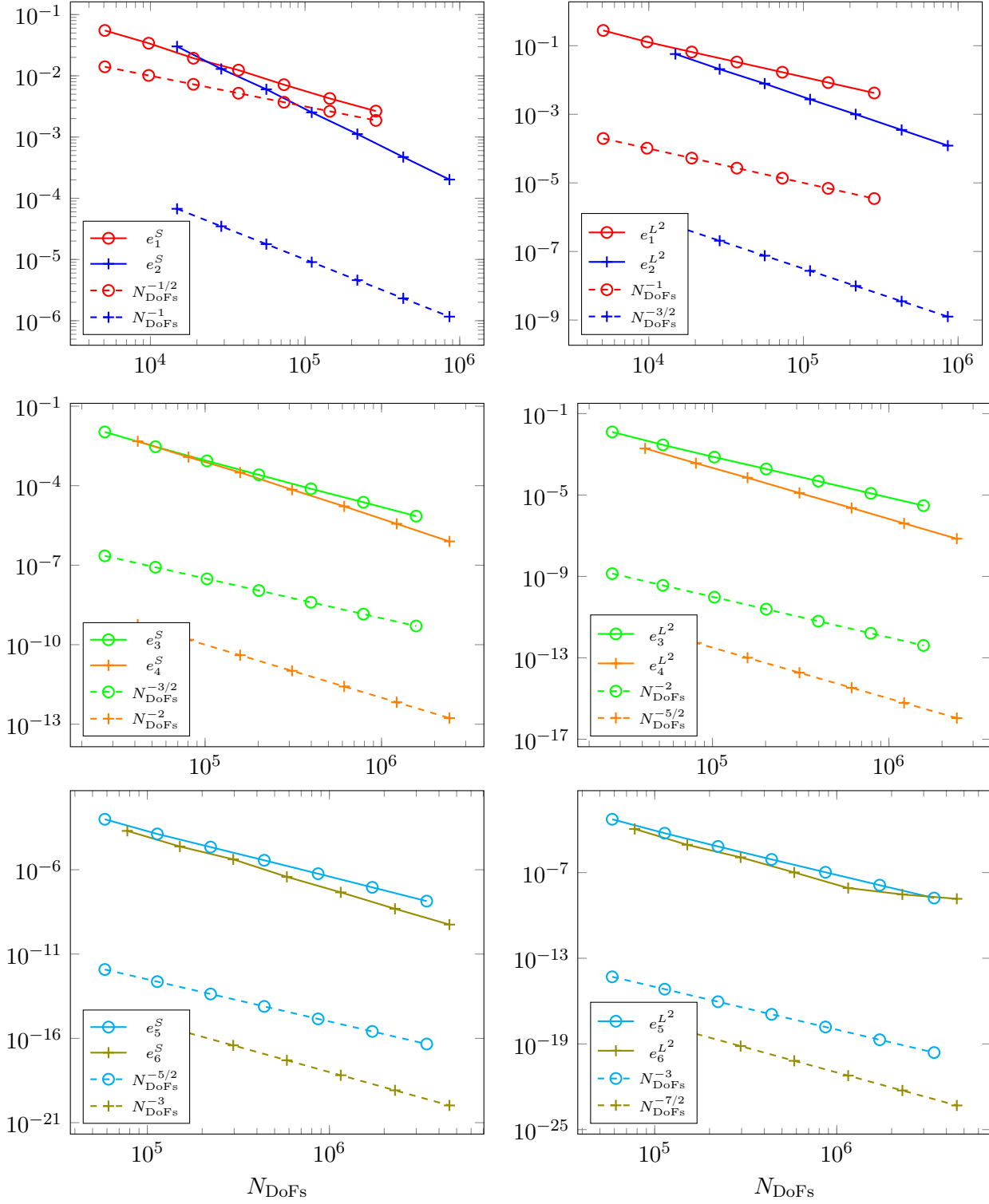


FIGURE 6. Second test case: logarithmic plot of the energy norm error e_m^S for increasing polynomial order $m = 1, \dots, 6$ and of the functions $N_{\text{DoFs}}^{-m/2}$ (dashed lines).

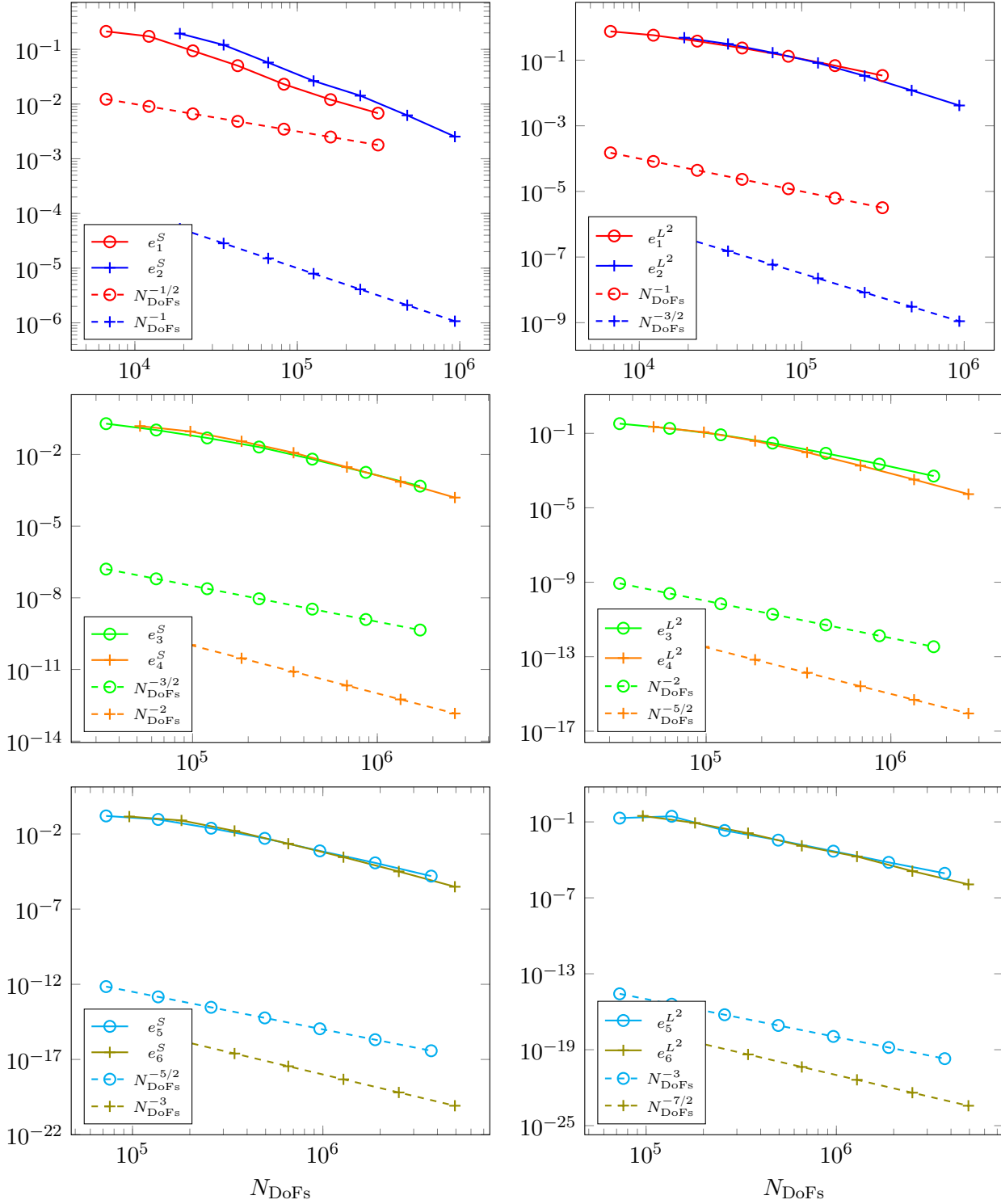


FIGURE 7. Third test case: logarithmic plot of the energy norm error e_m^S for increasing polynomial order $m = 1, \dots, 6$ and of the functions $N_{\text{DoFs}}^{-m/2}$ (dashed lines).